J. Phycol. **49,** 902–916 (2013)

DOI: 10.1111/jpy.12101

THREE NOVEL SPECIES IN THE *PSEUDO-NITZSCHIA PSEUDODELICATISSIMA* COMPLEX: *P. BATESIANA* SP. NOV., *P. LUNDHOLMIAE* SP. NOV., AND *P. FUKUYOI* SP. NOV. (BACILLARIOPHYCEAE) FROM THE STRAIT OF MALACCA, MALAYSIA[1]

Hong Chang Lim

Faculty of Resource Science and Technology, Universiti Malaysia Sarawak, Kota Samarahan, Sarawak 94300, Malaysia

Sing Tung Teng, Chui Pin Leaw

Institute of Biodiversity and Environmental Conservation, Universiti Malaysia Sarawak, Kota Samarahan, Sarawak 94300, Malaysia

and Po Teen Lim[2]

Faculty of Resource Science and Technology, Universiti Malaysia Sarawak, Kota Samarahan, Sarawak 94300, Malaysia

A study on the morphology and phylogeny of 18 strains of *Pseudo-nitzschia* established from the Strait of Malacca, Peninsular Malaysia, was undertaken. Morphological data combined with molecular evidence show that they constitute three new species, for which the names, *P. batesiana* sp. nov., *P. lundholmiae* sp. nov., and *P. fukuyoi* sp. nov., are proposed. The three new species closely resemble species in the *P. pseudodelicatissima* complex *sensu lato*. Morphologically, *P. batesiana* differs from other species in the complex by having a smaller part of cell overlapping in the chain, whereas *P. lundholmiae* differs by having fewer poroid sectors and *P. fukuyoi* by having a distinct type of poroid sectors. Nucleotide sequences of the LSU rDNA (D1–D3) of the three new species reveal significant nucleotide sequence divergence (0.1%–9.3%) from each other and from other species in the *P. pseudodelicatissima* complex *s.l.* The three species are phylogenetically closely related to species in the *P. pseudodelicatissima* complex, with *P. batesiana* appearing as a sister taxon to *P. circumpora*, *P. caciantha*, and *P. subpacifica*; whereas *P. lundholmiae* and *P. fukuyoi* are more closely related to *P. pseudodelicatissima* and *P. cuspidata*. The three species show 2–3 compensatory base changes (CBCs) in their ITS2 transcripts when compared to the closely related species. The ITS2 with its structural information has proven its robustness in constructing a better resolved phylogenetic framework for *Pseudo-nitzschia*.

Key index words: **ITS; LSU rDNA; morphology; *P. batesiana* sp. nov.; *P. fukuyoi* sp. nov.; *P. lundholmiae* sp. nov.; *Pseudo-nitzschia***

***Abbreviations*: ASP, amnesic shellfish poisoning; CBC, compensatory base change; DA, domoic acid; HCBC, hemi-compensatory base change; SNP, single-nucleotide polymorphism; TEM, transmission electron microscope**

The genus *Pseudo-nitzschia* Peragallo has gained considerable research attention due to its association with amnesic shellfish poisoning (ASP). Species in the genus are identified on the basis of the frustule's morphological features. Precise species identification is crucial; as one third of the species are known to produce the neurotoxin, domoic acid (DA) (Lundholm 2011, Lelong et al. 2012, Trainer et al. 2012), and the majority of DA-producing *Pseudo-nitzschia* spp. are reported as cosmopolitan (Hasle 2002).

Traditional species assignment was always difficult, which required taxonomic knowledge in conjunction with the technical skills on electron microscopy. A combination of molecular approaches has increasingly been applied to delimit species of *Pseudo-nitzschia* (Vrieling et al. 1996, Cho et al. 2001, Orsini et al. 2004, Cerino et al. 2005, McDonald et al. 2007, Quijano-Scheggia et al. 2010). Several molecular phylogenetic attempts have been made to reveal the lineages of *Pseudo-nitzschia* species, and to detect species limits by DNA sequence variation, yet, some taxonomic positions of closely related species remain elusive (e.g., *P. cuspidata* and *P. pseudodelicatissima*; Lundholm et al. 2012).

Cryptic and pseudo-cryptic species diversity of *Pseudo-nitzschia* has greatly complicated its taxonomy. Nevertheless, compelling evidence provided by various aspects of morphology, phylogenetic reconstruction, and sexual reproduction has allowed descriptions of novel species (e.g., Amato and Montresor 2008, Quijano-Scheggia et al. 2009, Lundholm et al. 2012). Lundholm et al. (2003) first suggested that *P. pseudodelicatissima* [Hasle] Hasle emend. Lundholm, Hasle and Moestrup was a complex when they revealed several pseudo-cryptic species with close morphological resemblances and phylogenetic relationships, and later described or emended

[1]Received 29 December 2012. Accepted 12 June 2013.
[2]Author for correspondence: e-mails: ptlim@frst.unimas.my, poteenlim@gmail.com.
Editorial Responsibility: O. De Clerck (Associate Editor)

the species as *P. pseudodelicatissima*, *P. cuspidata* [Hasle] Hasle, *P. caciantha* Lundholm, Moestrup and Hasle and *P. calliantha* Lundholm, Moestrup and Hasle. In the *P. pseudodelicatissima* complex *sensu lato*, another pseudo-cryptic species, *P. mannii* Amato and Montresor, was later described (Amato et al. 2007, Amato and Montresor 2008), and more recently, three new species were described, i.e., *P. hasleana* Lundholm, *P. fryxelliana* Lundholm (Lundholm et al. 2012), and *P. circumpora* Lim, Leaw and Lim (Lim et al. 2012a). It is apparent that the number of described species in this complex will increase, as new morphotypes continue to be discovered, especially from the Southeast Asian region, a shallow Sunda Shelf with tremendous marine biodiversity. Mollusc shellfish culture is intensively conducted along the coastlines of the Southeast Asian countries; occurrence of this potentially toxic species has posed a potential risk for ASP events in the region. This is evident by the recent detection of the ASP toxin, DA, in shellfish (Bajarias et al. 2006, Dao et al. 2006, 2009, 2012, Takata et al. 2009).

In Malaysian coastal waters, studies of *Pseudo-nitzschia* were initiated in 2007, in Kuching estuaries, the southeastern part of Borneo (Lim 2011, Su 2011, Lim et al. 2012b). Cell abundance of *Pseudo-nitzschia* in the study area, even though relatively low (data not shown), showed a high species diversity, with five species documented, including a new species, *P. circumpora* (Lim et al. 2012a). Our recent studies in the Strait of Malacca and the east coasts of Borneo revealed areas with tremendous *Pseudo-nitzschia* species richness, with 22 species recorded, plus a new morphotype closely resembling species in the *P. pseudodelicatissima* complex *s.l.* (Teng et al. 2013). Several other morphotypes with clear distinctive morphological features were also observed in the field samples; this finding prompted further investigations. The sampling sites were revisited for this study with the aim to establish clonal cultures of the morphotypes. Detailed morphological investigations were performed and molecular data were obtained. Frustule features and their morphometric measurements as well as the molecular data using the nuclear-encoded large subunit ribosomal DNA (LSU rDNA) and the internal transcribed spacers (ITS) region, indicated that the cultured strains comprised three new morphotypes; here described as *Pseudo-nitzschia batesiana* sp. nov., *P. lundholmiae* sp. nov., and *P. fukuyoi* sp. nov.

MATERIALS AND METHODS

Samples and culture collection. Plankton samples were collected from the west coast of Peninsular Malaysia: Teluk Batik, Perak (4.1886° N, 100.6052° E; Table S1 in the Supporting Information) using a 10 μm mesh size plankton net. Live samples were used for cell isolation, and parts were preserved with acidic Lugol's solution. Single cells or chains of *Pseudo-nitzschia* species were isolated under an Olympus IX51 inverted light microscope (Olympus, Tokyo, Japan) with a finely drawn Pasture pipette. Clonal cultures were established and maintained at 25°C (±0.5°C), at 12:12 h light:dark (L:D) photoperiods and an irradiance of 100 μmol photons $\cdot$ m^{-2} $\cdot$ s^{-1} in a temperature-controlled cold-white fluorescent incubator (SHEL LAB, Cornelius, OR, USA). Cultures were grown in SWII medium (Iwasaki 1961), salinity of 30 filtered natural seawater as a medium base, and enriched with 500 μM sodium metasilicate. The pH was adjusted to 7.8–7.9.

Morphological observation. Culture specimens were examined under LM using a Nikon Eclipse 80 light microscope, equipped with a Digital Sight DS-L1 digital camera (Nikon, Tokyo, Japan). The percentage of cell overlapping was determined and digital images were captured.

For transmission electron microscope (TEM), samples were acid cleaned as in Lim et al. (2012a). A few drops of cleaned material were mounted on Formvar-coated copper grids, dried, and examined under a JEOL JEM-1230 transmission electron microscope (JEOL, Tokyo, Japan). TEM micrographs were taken using Gatan Digital Micrograph (DM) software with an Erlangshen ES500W camera (Gatan, Pleasanton, CA, USA). Morphometric measurements were performed on the TEM images. Valve width, density of fibulae and striae, and types of poroids (Table S2 in the Supporting Information) were measured at the middle of the valve. Detailed morphology of cingular bands was also observed. Approximately 30 valves of each strain were randomly selected and used for morphometric measurement.

DNA extraction, amplification, and sequencing of rDNA. *Pseudo-nitzschia* cultures in mid exponential growth phase were harvested by centrifugation and the DNA was extracted as in Lim et al. (2012a). The internal transcribed spacer region (a region comprises ITS1, 5.8S rDNA, and ITS2; here refers as ITS region) was amplified using the primer pair, ITS1 and ITS4 (White et al. 1990, Lim et al. 2012c). The LSU rDNA in the domain 1–3 (D1–D3) was amplified using the primer pair, D1R and D3Ca (Scholin et al. 1994, Lim et al. 2012a).

Amplicons were purified using the Wizard® PCR Preps DNA Purification kit (Promega, Madison, WI, USA) according to the manufacturer's instructions. Purified amplicons were sequenced using the same primer pairs. Sequencing for each sample was performed on both strands by AIT Biotech (Singapore) on an ABI 3730XL DNA Analyzer (PE Biosystems, Vernon Hills, IL, USA).

ITS and LSU rDNA phylogenetic analyses. Nucleotide sequences of the ITS region obtained in this study and sequences of *Pseudo-nitzschia* retrieved from NCBI nucleotide database were aligned with T-Coffee (Notredame et al. 2000). A total of 68 operational taxonomic units (OTUs) were aligned, with *Fragilariopsis nana* [Steemann Nielsen] Paasche as the outgroup (Table S3 in the Supporting Information). Blocks of unreliable alignment were removed using GBlocks with default setting (http://molevol.cmima.csic.es/castresana/Gblocks_server.html; Castresana 2000, Talavera and Castresana 2007). The resulting alignment obtained from GBlocks was further edited manually using BioEdit Sequence Alignment Editor v7.0.9.0 (Hall 1999).

For LSU rDNA dataset, sequences were aligned using T-Coffee, and edited manually using BioEdit. The alignment comprises 66 OTUs, with five outgroup taxa: *Amphora coffeaeformis* [Agardh] Kützing, *Bacillaria paxillifer* [Müller] Hendey, *Cylindrotheca closterium* [Ehrenberg] Reimann and Kingston, *Nitzschia navis-varingica* Lundholm and Moestrup, and *Phaeodactylum tricornutum* Bohlin.

Alignments were submitted to TreeBASE with the study accession 14069 (http://purl.org/phylo/treebase/phylows/study/TB2:S14069) and the concatenated data sets were included in Appendix S1 in the Supporting Information. The

data sets were subjected to maximum parsimony (MP) and maximum likelihood (ML) analyses using PAUP* 4b10 (Swofford 2001), and Bayesian inference analyses (BI) using MrBayes v3.2.1 (Huelsenbeck and Ronquist 2001).

MP were carried out using heuristic searches with random addition of sequences (1,000 replications), branch-swapping with tree-bisection reconnection (TBR), and 1,000 bootstrap replicates (10 random addition of sequence run per bootstrap replicate). A substitution and rate heterogeneity model was selected using Akaike information criterion (AIC) as implemented in jModelTest 2 (Posada 2008). ML was performed using the most optimal model, starting with 100 random-addition replications; a heuristic search was made using TBR, and branch swapping. Bootstrap replications of 100 with 1 random addition of sequence run per bootstrap replicate were set. Corrected pair-wise distances (*p*-distances) were calculated, with parameters set according to the best model.

BI was performed with the model selected using Bayesian information criterion (BIC) (using jModelTest2). A four-chain run for 1,500,000 generations was used and trees were sampled every 100 generations. Posterior probabilities (PP) were estimated with 3,750 generations burn-in, and a majority rule consensus tree was constructed.

ITS2 transcript phylogenetic analyses. Secondary structure of the ITS2 transcript was modeled prior to multiple sequence structure alignment. The *Pseudo-nitzschia* ITS2 sequence start and end were annotated by identifying a 21-nucleotide interaction of the 5′ end of the 5.8S rRNA and the 3′ end of the LSU rRNA.

Folding and prediction of secondary structures of *Pseudo-nitzschia* ITS2 transcript were performed as described in Lim et al. (2012a). Only models with highest percentages of helix transfer were selected (threshold: 75%) in homologous modeling using ITS2 Database III (Schultz et al. 2006, Selig et al. 2008, Koetschan et al. 2009). For particular suboptimal regions, helices were refolded using RNAstructure ver. 5.02 (Mathews et al. 2004).

Orthologous alignment of the *Pseudo-nitzschia* ITS2 sequences was then obtained by synchronously aligning the nucleotide sequences with the secondary structure information using 4SALE (Seibel et al. 2006, 2008). CBC table was obtained from CBC matrix features in 4SALE. The ITS2 transcripts of species in the *P. pseudodelicatissima* complex were compared manually to identify CBCs and hemi-compensatory base changes (HCBCs). Signature sequences for the three new species found in Malaysian waters were identified from the sequence structure alignment. The sequences were displayed using WebLogo 3.3 (http://weblogo.threeplusone.com/create.cgi; Crooks et al. 2004). Secondary structures of ITS2 transcript were illustrated by VARNA (Darty et al. 2009). Phylogenetic analysis was performed as in Lim et al. (2012a).

RESULTS

Eighteen strains of *Pseudo-nitzschia* spp. collected from Teluk Batik, east coast of Peninsular Malaysia, were established (Table S1). Light and EM observation of the strains indicated a close resemblance to species in the *P. pseudodelicatissima* complex, which called for a further detailed morphological investigation and characterization of their rDNA. Both morphological and molecular data revealed significant degrees of morphological variation and genetic heterogeneity compared to previously described *Pseudo-nitzschia* species. Below, the differences found among strains and three new species are described as *Pseudo-nitzschia batesiana* sp. nov., *P. lundholmiae* sp. nov., and *P. fukuyoi* sp. nov.

Pseudo-nitzschia batesiana H. C. Lim, S. T. Teng, C. P. Leaw, and P. T. Lim **sp. nov.** (Fig. 1, A–I; Table S2)

Type locality: The west coast of Peninsular Malaysia (the Strait of Malacca), Teluk Batik, Perak, Malaysia (4.1886° N and 100.6052° E), collected on March 14, 2012.

Holotype: Acid-washed material of strain PnTb19 is deposited at the Microalgae Culture Collection of Universiti Malaysia Sarawak as permanent slide, with slide number assigned to A6-126-6a.

Isotype: Fixed material of PnTb19 deposited at the Microalgae Culture Collection of Universiti Malaysia Sarawak, numbered as A6-126-6b.

Molecular characterization: Nucleotide sequences of ITS1-5.8S-ITS2 and D1-D3 of LSU rDNA of strain PnTb19 were deposited in GenBank with the accession KC147514 and KC147534.

Etymology: The species is named in honor of Stephen S. Bates, Canada, for his contribution to diatom (Bacillariophyceae) and toxicity of *Pseudo-nitzschia* in particular.

Morphology: Cells are lanceolate and symmetrical in valve view and linear-lanceolate in girdle view (Fig. 1A); with 1/10 of cells overlapping in girdle view (Fig. 1B). A large central interspace with a central nodule is present (Fig. 1C). Cells are 84–86 μm long and 1.8–2.2 μm wide. The valve apices are rounded (Fig. 1D). One row of poroids is found in each stria, with five to six poroids in 1 μm (Fig. 1, C and F). The poroid hymens are divided into two to three sectors (Fig. 1E). The density of fibulae and striae is 15–19 and 29–32, respectively, in 10 μm; fibulae are irregularly spaced (Fig. 1F). Cingulum comprised three girdle bands, i.e., valvocopula, second, and third band (Fig. 1, G and H). The density of band striae in the valvocopula is 40–43 in 10 μm (Fig. 1, G and I). Valvocopula striae are biseriate and 3–4 poroids high (Fig. 1, G and I). Band striae of the second band are biseriate and two poroids high (Fig. 1, G and I), and a single longitudinal row of poroids is seen in the third band (Fig. 1H). The perforation pattern is hexagonal.

Molecular signature: Synapomorphy in helix II to pseudo-helix IIa of ITS2 nuclear rDNA: 5′-TGC CCT TTC TTC GCT TGA ATT TTA CTA CAC A-3′ (31 bp). This sequence includes two HCBCs, three single-nucleotide polymorphisms (SNPs), and four insertions, which differentiate it from the most similar species, *P. caciantha*. It differs from *P. circumpora* by one CBC, one HCBC, one SNP, and two deletions. It is readily distinguished from *P. subpacifica* (Hasle) Hasle by one HCBC, four SNPs, and two deletions (Fig. 2A). A Blastn confirmatory test on the signature of *P. batesiana* showed that the closest hit was a parasite with an *E*-value of 0.39. The next five hits were three mammals, a higher plant and a

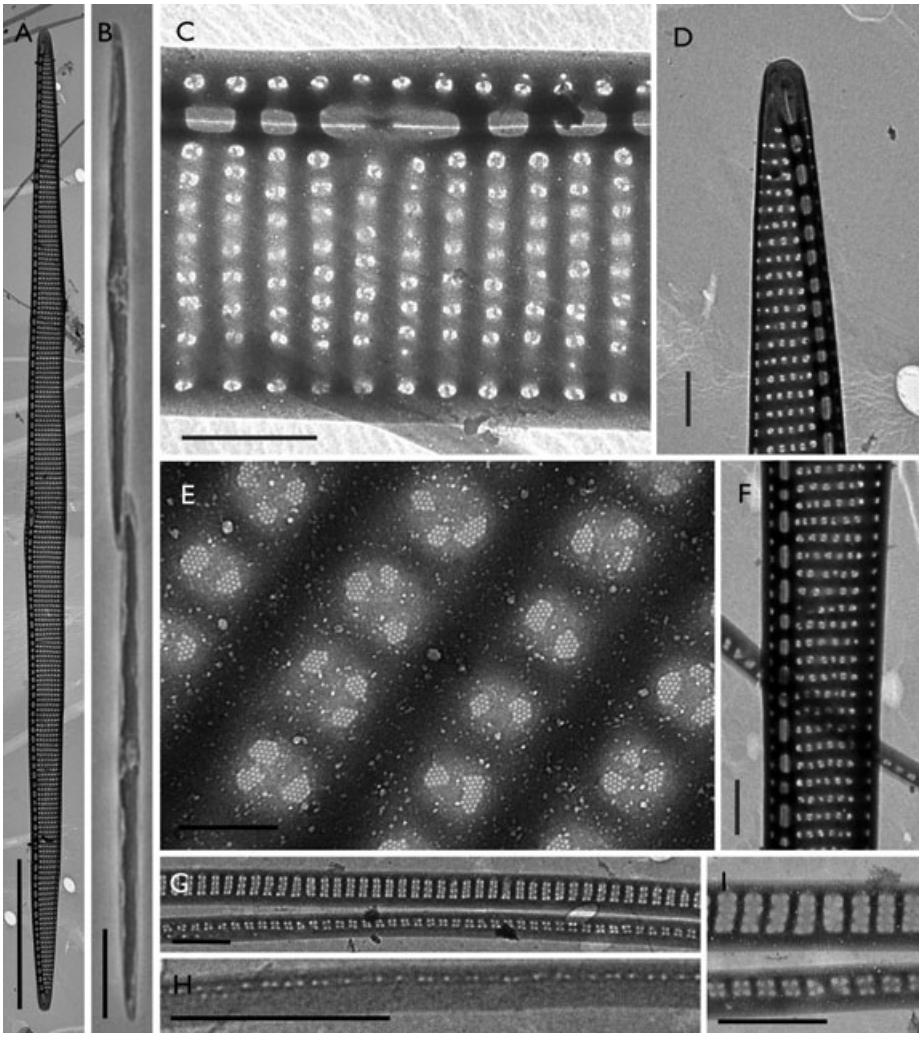

FIG. 1. *Pseudo-nitzschia batesiana* sp. nov. (A) Cell valve view, scale bar = 10 μm. (B) LM micrograph: Girdle view. Note cell overlap at 1/10; scale bar = 10 μm. (C) Striae, poroid structure of valve and mantle. Note central interspace; scale bar = 1 μm. (D) Valve ends; scale bar = 1 μm. (E) Detail of poroids. Note poroid hymen divided into two to three sectors. (F) Part of valve. Note irregularly spaced fibulae; scale bar = 1 μm. (G) Details of cingulum. Note valvocopula and second band; scale bar = 1 μm. (H) Detail of third band. (I) The close-up of valvocopula and second band; scale bar = 2 μm.

yeast (*E*-values of 1.6) (Blastn search performed on December 29, 2012).

Pseudo-nitzschia lundholmiae H. C. Lim, S. T. Teng, C. P. Leaw, and P. T. Lim **sp. nov.** (Fig. 3, A–H; Table S4 in the Supporting Information)

Type locality: The west coast of Peninsular Malaysia (the Strait of Malacca), Teluk Batik, Perak, Malaysia (4.1886° N, 100.6052° E), collected on March 14, 2012.

Holotype: Acid-washed, fixed material of strain PnTb10 is deposited at the Microalgae Culture Collection of Universiti Malaysia Sarawak as permanent slide, with slide number assigned to A6-126-3a.

Isotype: Fixed material of PnTb10 deposited at the Microalgae Culture Collection of Universiti Malaysia Sarawak, numbered as A6-126-3b.

Molecular characterization: Nucleotide sequences of ITS1-5.8S-ITS2 and D1-D3 of LSU rDNA of strain PnTb10 were deposited in GenBank with the accession KC147523 and KC147538.

Etymology: The species is named in honor of Nina Lundholm, Denmark, for her contributions to diatom taxonomy, especially *Pseudo-nitzschia* and Bacillariaceae.

Morphology: Cells are lanceolate, symmetrical in valve view (Fig. 3A), and slightly sigmoidal in girdle view, forming stepped colonies with 1/6 of cell overlapping (Fig. 3B). A central interspace with a central nodule is present (Fig. 3, A, C, H). Cells are 63–73 μm long and 1.7–2.3 μm wide (Table S2). Apices are rounded (Fig. 3, A and D). The number of fibulae and striae is 16–18 and 28–34, respectively, in 10 μm (Table S2). Fibulae are irregularly spaced (Fig. 3, A, H), and can be seen under LM. Striae consist of one row of round poroids, with 4–6 poroids in 1 μm (Fig. 3, C, E, F). Each poroid hymen is divided into 1–2 sectors, rarely three sectors were observed (3.3%, $n = 379$; Fig. 3, C, E, F). Some poroids are not divided into sectors (Fig. 3C). The perforation pattern of the sectors is hexagonal. The mantle is structured as valve face, being one poroid high. The density of band striae in valvocopula ranges from 35 to 40 in 10 μm (Fig. 3G). Each band stria is one to two poroids wide and two to three poroids high (Fig. 3G). The perforation of poroid sectors in valvocopula is hexagonal.

Molecular signature: Synapomorphy in helix III of ITS2 of nuclear rDNA: 5′-GAG TTT TAA TAG TGA

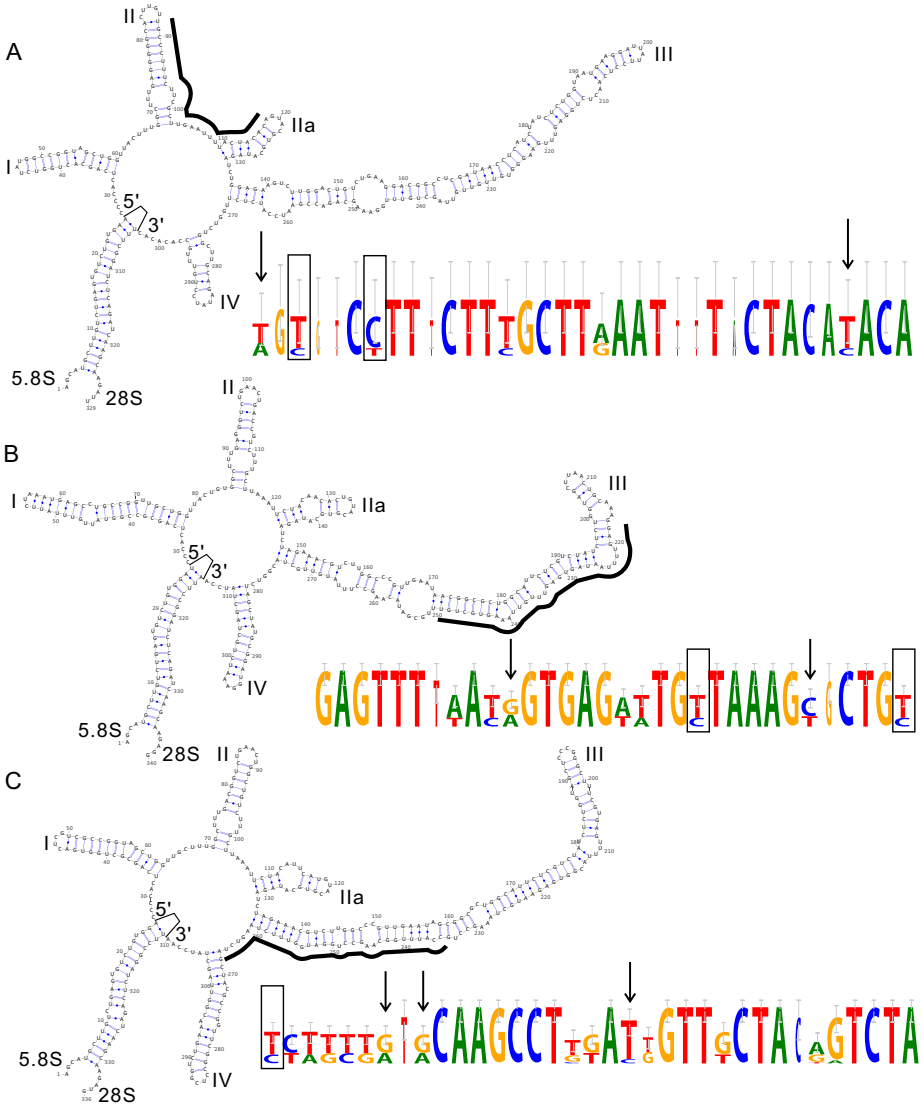

FIG. 2. Secondary structures of ITS2 and the molecular signatures of (A) *Pseudo-nitzschia batesiana*, (B) *P. lundholmiae*, and (C) *P. fukuyoi*. Rectangles indicate compensatory base changes (CBCs) and arrows point to hemi-compensatory base changes (HCBCs).

GTT TGT TAA AGT GCT GT-3′ (32 bp). This signature sequence includes a CBC, a HCBC, and six SNPs when compared with *P. fukuyoi*. It is distinguished from *P. cuspidata* by three SNPs, and from *P. pseudodelicatissima* by two HCBCs and one SNP (Fig. 2B). A confirmatory test of Blastn search in GenBank showed an *E*-value of 0.43 for the first four hits to chordata, followed by next three hits to mammals (*E*-value = 1.7) (Blastn search performed on December 29, 2012).

Pseudo-nitzschia fukuyoi H. C. Lim, S. T. Teng, C. P. Leaw, and P. T. Lim **sp. nov.** (Fig. 4, A–J; Table S2)

Type locality: The west coast of Peninsular Malaysia (the Strait of Malacca), Teluk Batik, Perak, Malaysia (4.1886° N, 100.6052° E), collected on March 14, 2012.

Holotype: Acid-washed, fixed material of strain PnTb25 is deposited at the Microalgae Culture Collection of Universiti Malaysia Sarawak as permanent slide with slide number assigned to A6-126-10a.

Isotype: Fixed material of PnTb25 deposited at the Microalgae Culture Collection of Universiti Malaysia Sarawak, numbered as A6-126-10b.

Molecular characterization: Nucleotide sequences of ITS1-5.8S-ITS2 and D1-D3 of LSU rDNA of strain PnTb25 were deposited in GenBank with the accession KC147516 and KC147535.

Etymology: The species is named in honor of Yasuwo Fukuyo, Japan, in recognition of his contributions to HABs, especially in the Western Pacific region (WESTPAC).

Morphology: Cells are linear to lanceolate, and symmetrical in valve view, slightly sigmoid in girdle view with pointed ends (Fig. 4A). Cells form stepped colonies with overlapping of 1/6 of total valve length (Fig. 4B). Apical and transapical axes are 74–81 μm and 1.5–1.9 μm, respectively (Table S2). A central interspace with a central nodule is present (Fig. 4, C and D). Proximal and distal mantle is similar to the valve, and one to two poroids high (one poroid high in distal mantle; Fig. 4, C and D). Parts of the

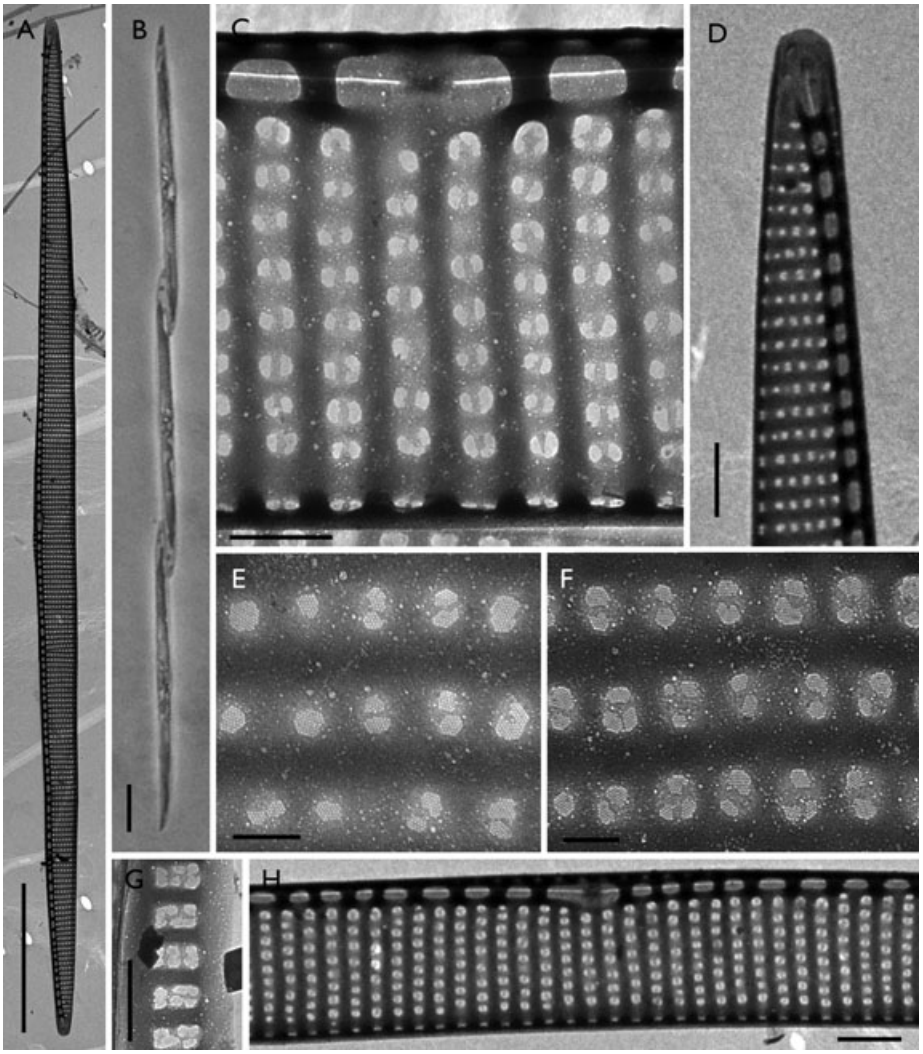

FIG. 3. *Pseudo-nitzschia lundholmiae* sp. nov. (A) Whole valve; scale bar = 10 μm. (B) LM micrographs: Girdle view. Note cell overlap at 1/6; scale bar = 10 μm. (C) Striae, poroid structure of valve and mantle. Note central interspace; scale bar = 0.5 μm. (D) Valve ends; scale bar = 1 μm. (E and F) Detail of poroids. Note poroids hymen with one to three sectors; scale bar = 0.2 μm. (G) Details of valvocopula; scale bar = 0.5 μm. (H) Valve striae structure; scale bar = 10 μm.

striae are composed of lightly silicified hymens, with no perforations (Fig. 4D). A lack of poroids in the weakly silicified stria at the end of both apices is also observed (Fig. 4E); while some have fine poroids (Fig. 4F). Fibulae are irregularly spaced, visible in LM, with a density of 17–19 in 10 μm; the density of striae ranged from 32 to 34 in 10 μm. Each stria comprises one row of round-square poroids, divided into two to three (rarely one) sectors (Fig. 4G). In addition, some of the poroids comprise four sectors (9.9%, $n = 528$; Fig. 4H). Rarely, a central sector in poroid hymen is observed. The perforation pattern is hexagonal in each sector. Poroids are spaced from four to six per 1 μm in each stria (Fig. 4, G and H). Cingulum comprises three bands, with valvocopula consisting of 39–47 band striae in 10 μm. Each band stria of the valvocopula is two poroids wide and three to four poroids high (Fig. 4I). The striae of the second band are biseriate with one row of poroids, while the third band structure only comprises one longitudinal row of poroids (Fig. 4J). The perforation in the cingular bands is hexagonal.

Molecular signature: Synapomorphy in between helix III and helix IV of ITS2 of nuclear rDNA: 5′-CCA TTT GGC AAG CCT GGA TGG TTT CTA AGT CTA-3′ (33 bp). This sequence includes a CBC that differentiated *P. fukuyoi* from *P. pseudodelicatissima* (additional four SNPs) and *P. cuspidata* (additional one HCBC and six SNPs). When compared to *P. lundholmiae*, a CBC, a HCBC, ten SNPs, and one insertion were found (Fig. 2C). A confirmatory test showed an *E*-value of 8e-09 for one *P. fukuyoi* sequence in GenBank (JN252420). The next five hits had *E*-value of 0.47 and were all sequences of mammals (Blastn search performed on December 29, 2012).

Taxonomic remarks: The two strains, PnKk36 and PnLk02, previously reported in Lim et al. (2012a) as *P. cuspidata* were reassigned to *P. fukuyoi* based on the morphological and genetics data.

Molecular data sets. The ITS alignment yielded a maximum individual sequence length of 936 nt, with a final alignment contained 1,436 columns. Of that, 514 columns were selected by GBlocks. The concatenated data matrix comprised 403 characters (28.1%); of which 236 were constant and 148 were

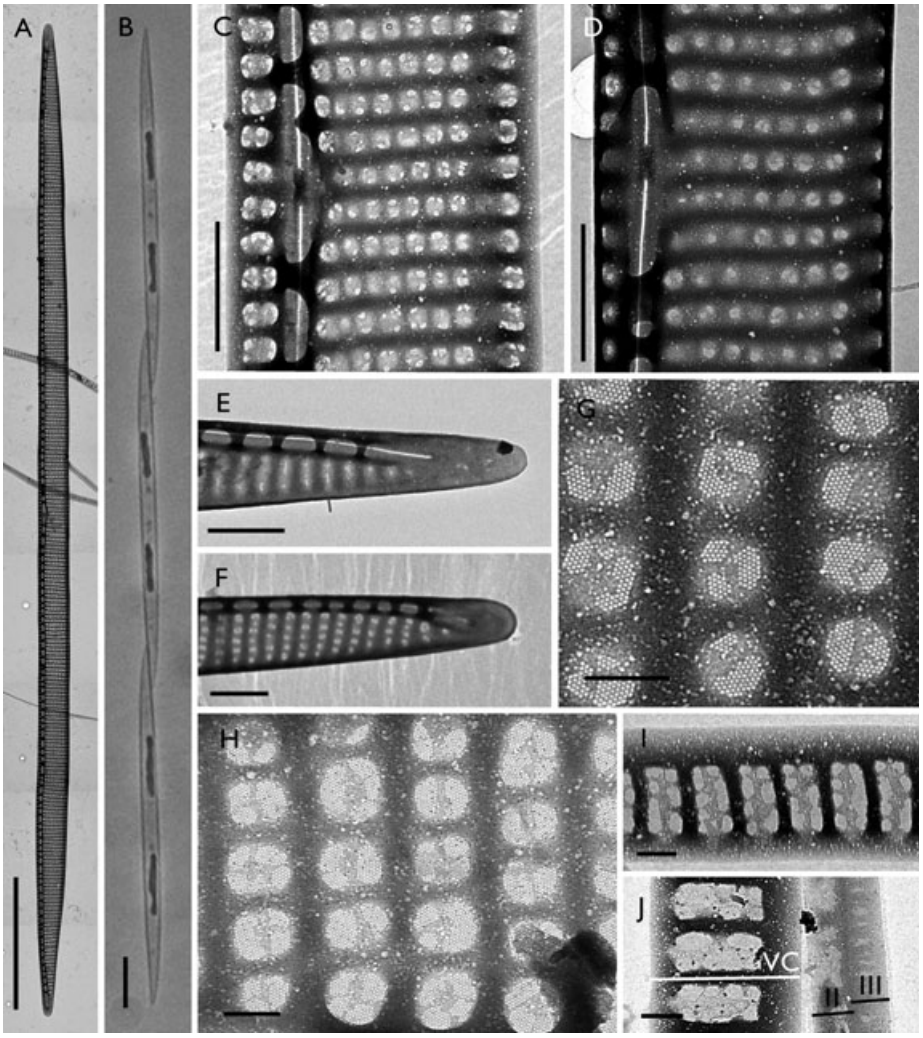

FIG. 4. *Pseudo-nitzschia fukuyoi* sp. nov. (A) Whole valve; scale bar = 10 μm. (B) LM micrograph: Girdle view. Note cell overlap at 1/6; scale bar = 10 μm. (C and D) Striae, poroid structure of valve and mantle. Note missing poroids and sectors; scale bar = 1 μm. (E and F) Valve ends with slightly different shapes; scale bar = 10 μm. (G and H) Detail of poroids. Note poroids hymens with two to four sectors; scale bar = 0.2 μm. (I) Details of valvocopula; scale bar = 0.2 μm. (J) The three cingular bands delimited by horizontal lines. From left: VC, valvocopula; II, second cingular band; III, third cingular band; scale bar = 0.2 μm.

parsimony informative. The remaining 71.9% of the positions (sites with insertions, deletions or gaps in the alignment) were excluded from further phylogenetic analyses.

The LSU rDNA alignment yielded 848 nt of maximum sequence length, with a final alignment contained 923 column. The alignment included 697 characters (75.5%), of which 136 were parsimony informative and 481 were constant. Corrected *p*-distances of the three new species compared to the closely related species are shown in Table S4.

The best substitution and rate heterogeneity models selected for ML analyses are as follows: SYM+I+G (parameter values set: rAC = 1.1076, rAG = 2.7038, rAT = 1.7603, rCG = 0.2560, rCT = 4.6690; *A*, *C*, *G* = equal; I = 0.4230; γ = 0.6860) for ITS data set, and TPM3uf+I+G (parameter values set: rAC = 0.3733, rAG = 2.4198, rAT = 1.0000, rCG = 0.3733, rCT = 2.4198; *A* = 0.2162, *C* = 0.2278, *G* = 0.3008; I = 0.4730; γ = 0.5000) for LSU rDNA data set. While the best model used in BI analyses are as follows: SYM+I+G (parameter values set as in ML) for ITS data set, and TPM3+I+G (parameter values set: rAC = 0.3434, rAG = 2.2071, rAT = 1.0000, rCG = 0.3434, rCT = 2.2071, rGT = 1.0000; *A*, *C*, *G* = equal; I = 0.4680; γ = 0.5120) for LSU rDNA data set.

Sequence structure alignment of *Pseudo-nitzschia* ITS2 transcripts yielded a maximum sequence length of 369 nt. The final alignment produced 612 columns; with 8.7% of the column as sequences at the proximal stem (5.8S-28S interaction).

Phylogenetic inferences. The phylogenetic analyses were performed with sequences from a very high number of *Pseudo-nitzschia* species: 32 species for the ITS analyses (~80% of the described species) and 27 species for the LSU rDNA analyses (~70% of the described species; Table S3). Three phylogenetic trees obtained from ITS (Fig. 5A), LSU rDNA (Fig. 5B) and ITS2 transcript (Fig. 6) were illustrated to evaluate the phylogenetic resolution of these genetic markers.

In ITS topology, *P. batesiana* made up a branch basal to a (*P. caciantha* + *P. subpacifica*), with strong node supports (MP/ML/BI, 96/94/1.00; Fig. 5A). In the LSU rDNA tree, *P. batesiana* appeared as a

taxon basal to a cluster comprising *P. circumpora* and (*P. caciantha* + *P. subpacifica*; Fig. 5B). This position is supported by the PNJ tree of ITS2 transcript, where *P. batesiana* also appeared basal to the same taxa: (*P. batesiana* (*P. caciantha* + *P. circumpora*) *P. subpacifica*); PP, 0.98; Fig. 6).

The phylogenetic analyses consistently revealed a highly supported grouping of (*P. fukuyoi* (*P. cuspidata* + *P. pseudodelicatissima*)), with *P. lundholmiae* as the sister taxon (Figs. 5 and 6).

It is interesting to note that the ribotype of *P. cuspidata*, Tenerife8, formed polytomy to *P. pseudodelicatissima* ribotype, P-11 (Lundholm et al. 2003), and other *P. pseudodelicatissima* strains (AL-15, 10A3 and Ner-D5 from Amato et al. 2007, Moschandreou et al. 2012, Orive et al. 2010) in our ITS tree (Fig. 5A). However, the phylogenetic position of *P. cuspidata* was resolved in the PNJ tree of ITS2 transcript, where the *P. cuspidata* ribotype, Tenerife8, was clustered with other *P. cuspidata* strains (AL-17 and Sydney1) and formed a sister clade to *P. fukuyoi* (Fig. 6).

Two Malaysian strains, PnKk36 (LSU rDNA sequence: JN252436) and PnLk02 (ITS sequence: JN252420) previously designated as *P. cuspidata* in Lim et al. (2012a), were genetically identical to *P. fukuyoi*. Both strains were clustered with *P. fukuyoi* in all topologies (ITS: MP/ML/BI, 99/100/1.00; LSU rDNA: MP/ML/BI, 56/54/0.90; ITS2 PNJ: PP, 1.00). Hence, the strains were reassigned as *P. fukuyoi*. Molecular distances among strains in the ITS2 data set of several species showed a degree of intraspecific divergence, with *P. cuspidata* being the highest (0.3%–4.6%) compared to *P. pseudodelicatissima* (0%–0.6%), *P. lundholmiae* (0%–0.3%), and *P. fukuyoi* (0%–1.2%). Interspecific genetic distances in the ITS2 region among the three new species and their closely related species are listed in Table S4. The pair-wise genetic distances of *P. batesiana*, *P. lundholmiae*, and *P. fukuyoi* with their sister species were in the range 10%–20%, which is in the range of divergence

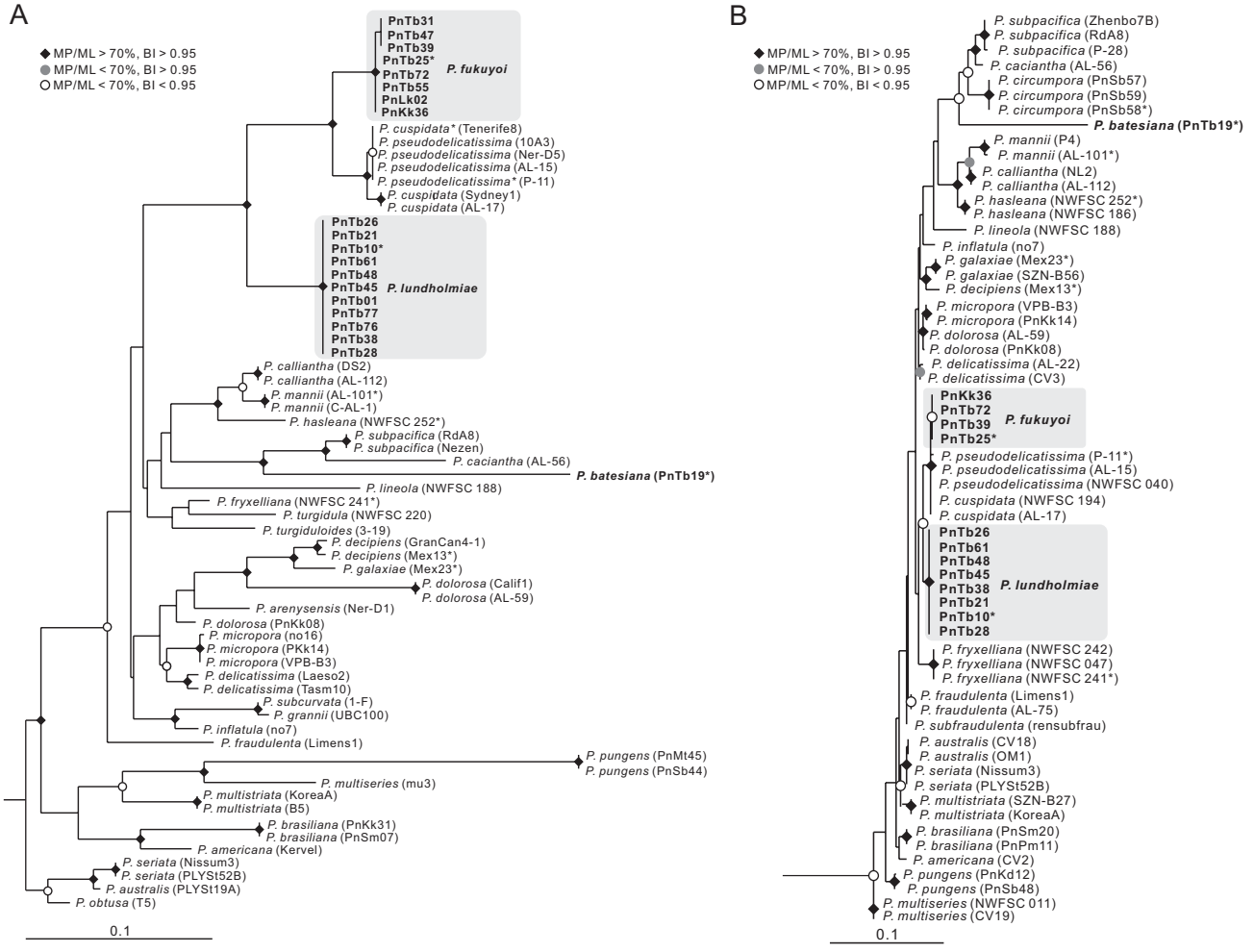

FIG. 5. (A) Phylogenetic tree from maximum likelihood (ML) analysis based on *Pseudo-nitzschia* whole ITS1-5.8S-ITS2 region of the ribosomal DNA (403 characters included). The tree is rooted (outgroup not shown). (B) Phylogenetic tree from ML analysis based on the *Pseudo-nitzschia* D1–D3 LSU rDNA (697 characters included). The tree is rooted (outgroup not shown). Asterisks indicate types strains used in species references. Both trees search used 100 random-addition replications and TBR branch swapping.

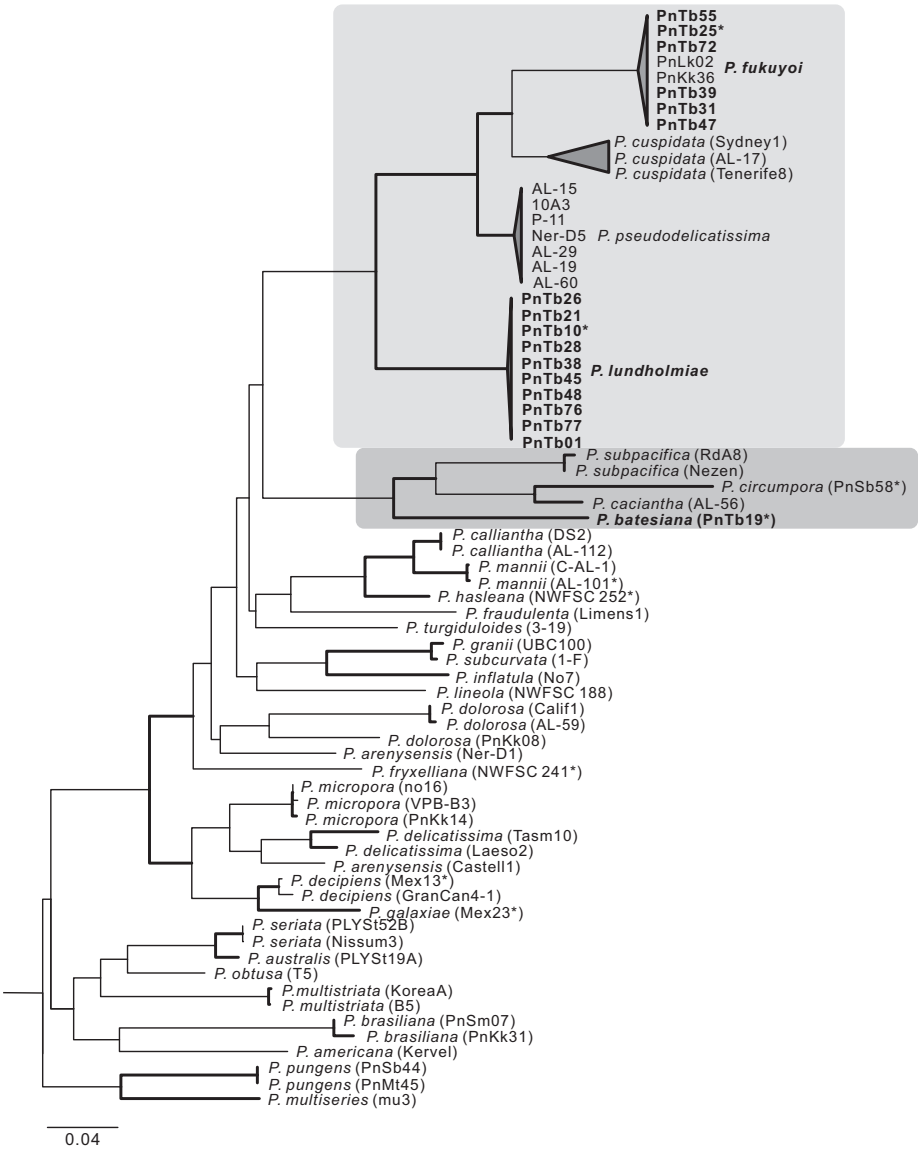

FIG. 6. Profile neighbor-joining tree based on ITS2 with orthologous sequence structure alignment information (612 positions included) using ProfDistS. The tree was rooted with *Fragilariopsis kerguelensis* (EF660061) as the outgroup. The nodal supports are bootstrap values from 1,000 pseudo-replications. Posterior probabilities of more than 95% are marked with thick lines.

observed between species: *P. cuspidata* and *P. pseudodelicatissima*: 0.3%–5.2%; *P. circumpora* and *P. caciantha*: 13.6%; and *P. caciantha* and *P. subpacifica*: 12.8%–13% (Table S4).

ITS2 secondary structures. Two types of secondary structures were observed in the ITS2 transcripts of *Pseudo-nitzschia* spp., viz. Type A and Type B. Type A transcript has a connected helix III and helix IV; while in type B, both helices are separated by a few base pairs. *Pseudo-nitzschia micropora* Prissholm and Moestrup, *P. delicatissima* (Cleve) Heiden, *P. arenysensis* Quijano-Scheggia, Garcés, Lundholm, *P. decipiens* Lundholm and Moestrup, *P. galaxiae* Lundholm and Moestrup, *P. seriata* (Cleve) Peragallo, *P. australis* Frenguelli, *P. obtusa* (Hasle) Hasle and Lundholm, *P. multistriata* (Takano) Takano, *P. brasiliana* Lundholm, Hasle and Fryxell, *P. americana* (Hasle) Fryxell, *P. pungens* (Grunow ex Cleve) Hasle, and *P. multiseries* (Hasle) Hasle are all in type A while the rest of the *Pseudo-nitzschia* species modeled in this study are type B. Generally, the transcripts comprised four helices (I–IV) and one pseudo-helix (IIa), similar to what has been recorded in previous studies (e.g., Amato et al. 2007, Casteleyn et al. 2008, Lim et al. 2012c). Numerical and statistical descriptions of the secondary structure information are given in Table S5 in the Supporting Information.

The average sequence length of ITS2 in *Pseudo-nitzschia* was 278 bp (254–316 bp). GC contents in the helices ranged from 35% to 52%. Secondary structure analyses and structural comparisons

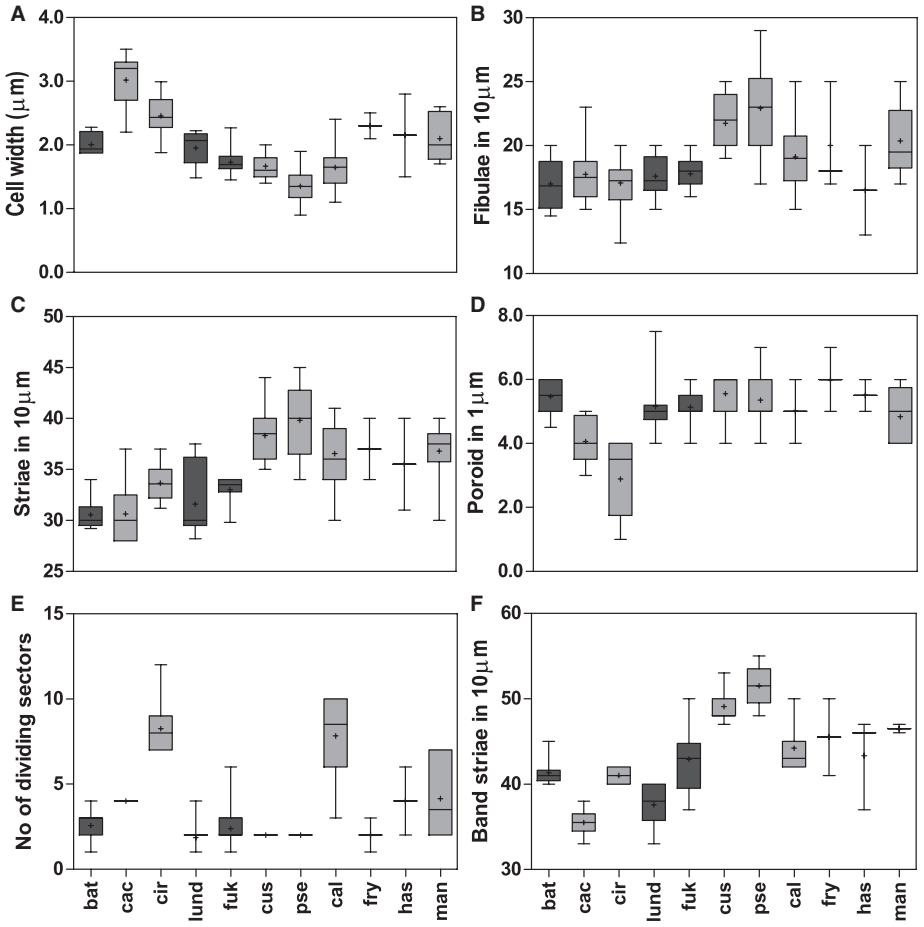

FIG. 7. Morphometric data on cell width (A), fibulae (B), striae (C), poroid (D), perforation sectors (E), and density of band striae (F) of species classified under the *Pseudo-nitzschia pseudodelicatissima* complex: *P. batesiana* (bat), *P. caciantha* (cac), *P. circumpora* (cir), *P. lundholmiae* (lund), *P. fukuyoi* (fuk), *P. cuspidata* (cus), *P. pseudodelicatissima* (pse), *P. calliantha* (cal), *P. fryxelliana* (fry), *P. hasleana* (has), and *P. mannii* (man). The data on *P. batesiana*, *P. lundholmiae*, and *P. fukuyoi* are from this study; data on *P. caciantha*, *P. calliantha*, *P. cuspidata*, and *P. pseudodelicatissima* are from Lundholm et al. (2003), Trainer et al. (2009), Moschandreou and Nikolaidis (2010), Lundholm et al. (2012); data on *P. fryxelliana* and *P. hasleana* are from Lundholm et al. (2012); and *P. mannii* from Amato and Montresor (2008). Boxes indicate the standard error, line in box indicates the median, + in box showed the mean while the whiskers showed the min and max. Dark gray boxed represent the three new species described in this study.

revealed that the structures are relatively conserved, despite large differences in the total nucleotide length (254–316 bp). U–U mismatch, the universal conserved motif, was in all ITS2 transcripts positioned at 8–18 paired bases in helix II. The conserved motifs UAAAU and UGGU were observed in all species. The UAAAU motif was found in the loop located between helix II and IIa, whereas the UGGU motif was located near the apex of helix III. A proximal stem of 5.8S-28S interactions was conserved with a range 17–21 paired bases.

Pair-wise structural comparisons of ITS2 transcripts between *P. batesiana*, *P. fukuyoi*, *P. lundholmiae* to the closely related species are summarized in Table S6 in the Supporting Information. Structural comparisons of *P. batesiana* to its sister species, *P. caciantha*, *P. circumpora*, and *P. subpacifica*, revealed two CBCs; and seven, eight, and nine HCBCs, respectively. The locations of CBCs, however, differed among species: in *P. caciantha* they were located in helix I and helix III; in *P. circumpora* in helix I and helix II; and in *P. subpacifica* in helix III and helix IV. Detailed positions of each HCBC are reported in Table S6.

Comparison between *P. lundholmiae* and (*P. cuspidata* and *P. pseudodelicatissima*) showed the presence of two CBCs, situated in helix I and helix IV. Ten HCBCs were identified between *P. lundholmiae* and *P. cuspidata* (see Table S6). A total of eight HCBCs were found between *P. lundholmiae* and *P. pseudodelicatissima*, with two in helix I, one in helix II, one in helix IIa, and four in helix III. ITS2 secondary structures of *P. fukuyoi* revealed the presence of two CBCs situated in helix III when compared to *P. cuspidata* and *P. pseudodelicatissima* (Table S6).

ITS2 transcripts of both *P. cuspidata* and *P. pseudodelicatissima* were also compared and showed the presence of one CBC (in helix IV) and five HCBCs (two in helix I and three in helix III). However, a comparison between ITS2 transcripts of *P. cuspidata*, Tenerife8 (AY257853), a strain isolated from waters closer to the type locality, Tenerife, Canary Island (Hasle, 1965), and *P. pseudodelicatissima*, P-11 (AF417640), isolated from Portugal, revealed only one HCBC.

DISCUSSION

Description of three novel species in the P. pseudodelicatissima *complex.* The description of pseudo-cryptic *P. batesiana*, *P. lundholmiae*, and *P. fukuyoi* is supported by morphological evidence and molecular data. Basically, the three species can be identified

based on several characteristics: percentage of cell overlap in live cells, valve width, number of sectors in poroids, densities of band striae, and structure of the valvocopula. *Pseudo-nitzschia batesiana* is distinguished from *P. lundholmiae* and *P. fukuyoi* under LM by having a 1/10 of cell overlap, compared to a 1/6 cell overlap in *P. lundholmiae* and *P. fukuyoi* (Figs. 1, 3 and 4). *Pseudo-nitzschia batesiana* tends to have a wider valve and lower striae density than *P. fukuyoi* (Fig. 7, A, C; Table S2). Although poroids of *P. batesiana* and *P. fukuyoi* are divided into two to three sectors, *P. fukuyoi* has a greater tendency to have four sectors (Figs. 1; 4; and 7E; Table S2). In addition, the structures of second and third band in *P. batesiana* differed from *P. fukuyoi*, distinctively (Figs. 1 and 4; Table S2). *Pseudo-nitzschia batesiana* is readily distinguished from *P. lundholmiae* by a higher number of dividing sectors, densities of band striae, and the variation in the structure of the valvocopula (Figs. 1; 3; and 7, E, F; Table S2). *Pseudo-nitzschia lundholmiae* differs from *P. fukuyoi* by having a tendency for fewer sectors in the poroids and lower densities of band striae (Figs. 3; 4; and 7, E, F; Table S2). In the structure of band striae, *P. lundholmiae* tend to have variable band striae, usually uniseriate or biseriate with two to three poroids high, whereas it is always biseriate, with three to four poroids high in that of *P. fukuyoi* (Figs. 3 and 4; Table S2).

At present, the *P. pseudodelicatissima* complex *s.l.* is defined specifically based on frustule morphology, i.e., *Pseudo-nitzschia* species with width <3 μm and each striae comprised with only one row of poroid (Lundholm et al. 2012). The complex comprises *P. caciantha*, *P. calliantha*, *P. circumpora*, *P. cuspidata*, *P. fryxelliana*, *P. hasleana*, *P. mannii*, and *P. pseudodelicatissima*. To discern the pseudocryptic species in this complex, several morphological characteristics are required. The number of poroid sectors, density of fibulae, striae and band striae, and structure of the valvocopula are among the important characters in delimiting the species in this complex. However, a considerable overlapping between several morphometric characters exists among the species in *P. pseudodelicatissima* complex *s.l.*, which in hand needed a detail and thorough comparison to delimit one from another.

The three new species all belong to this complex. Among the species in the complex, *P. batesiana* and *P. lundholmiae* morphologically resemble *P. cuspidata*, *P. pseudodelicatissima*, and *P. fryxelliana* the most (Lundholm et al. 2003, Trainer et al. 2009, Li et al. 2010), sharing the number of poroids in 1 μm (~4–6 poroids, Table S2) and a similar number of sectors (2–3, Table S2). The main morphological differences that characterize *P. batesiana* and *P. lundholmiae* compared to *P. cuspidata*, *P. pseudodelicatissima*, and *P. fryxelliana* are a lower density of fibulae, striae, and band striae (Table S2).

Morphologically, *P. batesiana* is akin to *P. fryxelliana* with respect to poroid sectors (two to three sectors); although only one sector was occasionally found in *P. fryxelliana* (Lundholm et al. 2012). Despite the similarity, *P. batesiana* is distinguished from *P. fryxelliana* because the latter has a lower density of fibulae, striae, and band striae (*P. batesiana*: 15–19, 29–32, 40–43 in 10 μm, compared to *P. fryxelliana* [17]18–25, 34–40, 41–50 in 10 μm; Fig. 7, B, C, F, Table S2; Lundholm et al. 2012). In addition, the valvocopula of *P. batesiana* is three to four poroids high, whereas it is one to three poroids high in *P. fryxelliana* (Lundholm et al. 2012). Genetically, *P. batesiana* is distinct from the others by a high degree of sequence divergence (8%–9% in the LSU rDNA), and it forms a well-supported sister taxon to *P. caciantha*, *P. subpacifica*, and *P. circumpora*. Concordant results were obtained in the structural comparison of the ITS2 transcripts, with at least two CBCs found between *P. batesiana* and its closely related species, *P. caciantha*, *P. circumpora*, and *P. subpacifica*.

Pseudo-nitzschia lundholmiae differs from *P. pseudodelicatissima* by its valve shape (*P. lundholmiae*, lanceolate; *P. pseudodelicatissima*, linear). The width is slightly larger in *P. lundholmiae* (1.7–2.3 μm) compared to *P. pseudodelicatissima* (0.9–1.6 μm; Lundholm et al. 2003). Furthermore, *P. lundholmiae* is distinguished from *P. pseudodelicatissima* and *P. fryxelliana* by having a lower density of fibulae and striae: *P. lundholmiae*, 16–18 and 28–34, respectively; *P. pseudodelicatissima*, 20–25 and 36–43, respectively (Lundholm et al. 2003); *P. fryxelliana* (17)18–25 and 34–40, respectively (Lundholm et al. 2012, Fig. 7, B, C; Table S2). The density of band striae is also lower in *P. lundholmiae* (40–43 in 10 μm) compared to *P. pseudodelicatissima* and *P. fryxelliana* (48–55 and 41–50, respectively, in 10 μm; Fig. 7F; Table S2). The morphological resemblance between *P. lundholmiae* to *P. pseudodelicatissima* is in accordance with our molecular phylogenetic inferences, where *P. lundholmiae* consistently formed a well-supported basal to *P. pseudodelicatissima*, *P. cuspidata*, and *P. fukuyoi*; albeit a rather low genetic variability in the LSU rDNA (1.0%–1.2%).

The valve ultrastructure of *P. fukuyoi* is similar to that of *P. caciantha*, *P. cuspidata*, *P. fryxelliana*, *P. hasleana*, *P. mannii*, and *P. pseudodelicatissima* (Lundholm et al. 2003, 2012, Amato and Montresor 2008). *Pseudo-nitzschia fukuyoi* differs from the others by having a narrower cell width (1.5–1.9 μm), compared to *P. caciantha* (2.7–3.5 μm), *P. fryxelliana* (2.1–2.5 μm), *P. hasleana* (1.5–2.8 μm), *P. mannii* (1.7–2.6 μm; Lundholm et al. 2003, Amato and Montresor 2008, Lundholm et al. 2012). An exception is *P. cuspidata*, which has an range of valve widths (1.4–2.0 μm; Lundholm et al. 2003) overlapping with *P. fukuyoi*. *Pseudo-nitzschia fukuyoi* and *P. caciantha* differ in their valve view; the former is symmetrical (Fig. 4), while the latter is asymmetrical

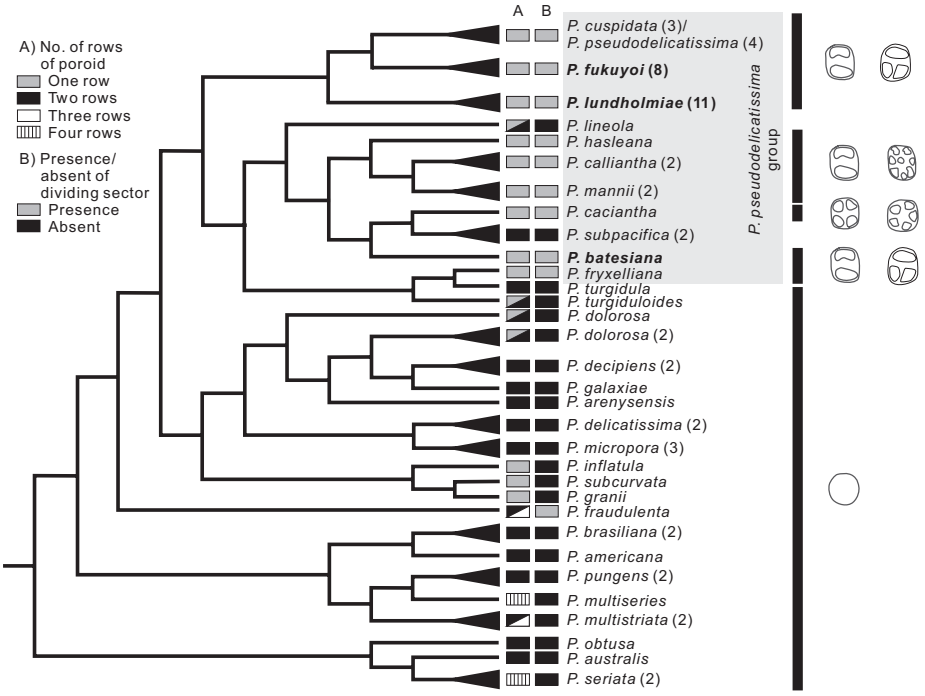

FIG. 8. Morphological characters mapped onto the ITS ML tree of *Pseudo-nitzschia*. Several clades were collapsed to triangles with the number on the right (in bracket) indicates the number of taxa. Drawings represent the number of dividing sectors.

(Lundholm et al. 2003). The most significant differences between *P. fukuyoi* and *P. caciantha* are the density of striae (32–34 in *P. fukuyoi*; 28–31 in *P. caciantha*), density of poroids in striae (5–6 in *P. fukuyoi*; 3.5–5 in *P. caciantha*), numbers of sectors (2–3 [4] in *P. fukuyoi*; 4–5 in *P. caciantha*), and the density of band striae (39–47 in *P. fukuyoi*; 33–38 in *P. caciantha*; Lundholm et al. 2003). Cells of *P. fukuyoi* have a lower density of fibulae and striae (17–19 and 32–34) compared to *P. cuspidata* (19–25 and 35–44, Lundholm et al. 2003) and *P. fryxelliana* ([17]18–25 and 34–40, Lundholm et al. 2012); and a fewer poroid sectors than *P. hasleana* and *P. mannii* (Amato and Montresor 2008, Lim et al. 2012a, Table S2). Even though the number of sectors in poroids of *P. fukuyoi* and *P. cuspidata* is almost the same, *P. cuspidata* does not possess poroids with central sectors (Lundholm et al. 2003, Trainer et al. 2009).

To further evaluate taxonomic-informative morphological characters of the three new species, two characters *viz.* the number of rows of poroids (character A) and the presence/absence of dividing sectors in the poroid (character B), were mapped onto the ML ITS tree (Fig. 8). These two morphological characteristics have been considered important features that split *P. pseudodelicatissima* complex from other complexes; however, the character state evolution did not reflect morphological congruency, with homoplasies observed in *P. lineola* (Cleve) Hasle and *P. subpacifica*.

Nucleotide sequence alignment strategies. Different alignment strategies were implemented in this study to infer the phylogenetic relationship of *Pseudo-nitzschia* from the selected genetic markers, i.e., ITS, LSU rDNA, and the ITS2 transcript, with the aim to resolve the phylogenetic ambiguity, particularly species in the *P. pseudodelicatissima* complex *s.l.*

Alignment of the whole region of ITS is always difficult; not only in the group of *Pseudo-nitzschia* but also other diatom species, such as *Sellaphora* (Behnke et al. 2004). As such the highly variable ITS data set of *Pseudo-nitzschia* was aligned with T-Coffee and further analyzed by GBlocks to gain a better alignment for phylogenetic reconstruction. On the other hand, the conserved LSU rDNA data set is readily aligned by T-Coffee. For a nucleotide region with high sequence variability, orthologous sequence alignment is always crucial, and sometimes this can be improved by incorporating the structural information into the alignment (e.g., Alverson et al. 2006, Keller et al. 2010). In this study, sequence structure alignment was performed on ITS2 data set, and used in reconstructing the phylogenetic tree. Inclusion of secondary structural information into the reconstructed phylogenetic tree has been demonstrated with better bootstrap support due to the increased number of states (Keller et al. 2010). This is also demonstrated in the study with a 1-fold increase of number of columns in our sequence structure alignment.

The secondary structures of *Pseudo-nitzschia* ITS2 transcripts were confirmed by observing the ITS2-proximal stem (5.8S-28S interactions), this region is well conserved in its sequence and secondary structure, as demonstrated in green algae (Mai and Coleman 1997), yeast (Peculis and Greer 1998), dinoflagellates (Gottschling and Plötner 2004),

flowering plants (Koetschan et al. 2010), and blue butterfly (Wiemers et al. 2009).

Is ITS2 transcript a better marker to resolve Pseudo-nitzschia *phylogeny?* Presence of CBC in the ITS2 transcript helps distinguishing among biologically distinct but morphologically similar species (Ruhl et al. 2010). Our pair-wise CBCs comparisons showed that distinct morphospecies possess at least one CBC; further supports CBC information as a useful classifier in *Pseudo-nitzschia* taxonomy, particularly when cryptic and pseudo-cryptic species diversity is considerably high (Amato et al. 2007, Müller et al. 2007, Lim et al. 2012a, this study). Mating experiment coupled with CBCs data had been used to discriminate pseudo-cryptic *P. mannii* in the *P. pseudodelicatissima* complex (Amato and Montresor 2008). Later, the cryptic *P. arenysensis* in the *P. delicatissima* complex were described based on the same species recognition (Quijano-Scheggia et al. 2009). The recognition was well accepted in other algal groups, and further demonstrated the correlation of CBCs in ITS2 transcript with the reproductive isolation (i.e., *Closterium ehrenbergii* Meneghini ex Ralfs, Ichimura and Kasa 1995, *Sellaphora pupula* (Kütz.) Mereschk, Behnke et al. 2004). However, it is important to emphasize here that CBCs are correlated with species distinction, and the fundamental of novel species description will still rely on the decision of taxonomist (Alverson 2008, Coleman 2009).

The pseudo-cryptic species *P. pseudodelicatissima* and *P. cuspidata*, morphologically differ only by their valve shape, with the former being linear and the latter lanceolate (Lundholm et al. 2003). Over the years, molecular techniques have attempted to discriminate the two species. Recently, the genetic data obtained from strain Tenerife8 were suggested to be the reference data for *P. cuspidata* (Lundholm et al. 2012). But a distinction between the two species remains unresolved using LSU rDNA analyses (Amato et al. 2007, Lim et al. 2012a, this study), the ITS region (Lundholm et al. 2003, 2006, Orive et al. 2010, Lundholm et al. 2012, this study), and ITS2 sequences (without incorporating structural information) (Amato and Montresor 2008). In our ITS2 transcript PNJ tree, the strains identified as *P. pseudodelicatissima* and *P. cuspidata* appeared as two well-resolved clades (Fig. 6). Incorporation of secondary structure in phylogenetic reconstruction has been proven its accuracy and robustness (Keller et al. 2010). Our analysis therefore once again demonstrates the feasibility and effectiveness of using ITS2 transcripts as a tool for discriminating, *P. pseudodelicatissima* and *P. cuspidata*, as well as species in *P. pseudodelicatissima* complex.

Conclusion. Over the past 2 years, extensive sampling of coastal waters of Malaysia and the establishment of *Pseudo-nitzschia* species into culture have yielded new morphotypes, and new species have been described (Lim et al. 2012a). We performed phylogenetic analyses on three genetic data sets that differed greatly in the alignment strategies. ITS2 sequence structure alignment was once again proven to improve the accuracy of alignment and robust phylogenetic framework. It is notable that *P. pseudodelicatissima*-like diatoms isolated from this region have revealed three new morphotypes as well as genotypes. This might be a forewarning that, new species will be continued to be uncovered, especially in this region, where fewer studies have been performed. The three new species described herein are evidently supported by both morphological and molecular data. Their ability to produce DA, however, remains unknown.

The authors are grateful to Stephen S. Bates and Nina Lundholm for the valuable suggestions and English revision of the manuscript. We also thank two anonymous reviewers for critical comments and suggestions. This paper forms part of the Ph.D. project of H.C. Lim, supported by the Malaysian Ministry of Higher Education (MoHE) through a MyBrain15 MyPhD scholarship. This work was funded by the Malaysian Government through MOSTI ScienceFund 04-01-09-SF0092, MoHE Malaysian-JSPS Matching Fund, and RACE.

Alverson, A. J. 2008. Molecular systematics and the diatom species. *Protist* 159:339–53.

Alverson, A. J., Cannone, J. J., Gutell, R. R. & Theriot, E. C. 2006. The evolution of elongate shape in diatoms. *J. Phycol.* 42:655–68.

Amato, A., Kooistra, W. H. C. F., Ghiron, J. H. L., Mann, D. G., Pröschold, T. & Montresor, M. 2007. Reproductive isolation among sympatric cryptic species in marine diatoms. *Protist* 158:193–207.

Amato, A. & Montresor, M. 2008. Morphology, phylogeny, and sexual cycle of *Pseudo-nitzschia mannii* sp. nov. (Bacillariophyceae): a pseudo-cryptic species within the *P. pseudodelicatissima* complex. *Phycologia* 47:487–97.

Bajarias, F. F. A., Kotaki, Y., Relox, J. R., Jr, Romero, M. L. J., Furio, E. F., Lundholm, N., Koike, K., Fukuyo, Y. & Kodama, M. 2006. Screening of diatoms producing domoic acid and its derivatives in the Philippines. *Coast. Mar. Sci.* 30:121–9.

Behnke, A., Friedl, T., Chepurnov, V. A. & Mann, D. G. 2004. Reproductive compatibility and rDNA sequence analyses in the *Sellaphora pupula* species complex (Bacillariophyta). *J. Phycol.* 40:193–208.

Casteleyn, G., Chepurnov, V. A., Leliaert, F., Mann, D. G., Bates, S. S., Lundholm, N., Rhodes, L., Sabbe, K. & Vyverman, W. 2008. *Pseudo-nitzschia pungens* (Bacillariophyceae): a cosmopolitan diatom species? *Harmful Algae* 7:241–57.

Castresana, J. 2000. Selection of conserved blocks from multiple alignments for their use in phylogenetic analysis. *Mol. Biol. Evol.* 17:540–52.

Cerino, F., Orsini, L., Sarno, D., Dell'Aversano, C., Tartaglione, L. & Zingone, A. 2005. The alternation of different morphotypes in the seasonal cycle of the toxic diatom *Pseudo-nitzschia galaxiae*. *Harmful Algae* 4:33–48.

Cho, E. S., Park, J. G., Oh, B. C. & Cho, Y. C. 2001. The application of species specific DNA-targeted probes and fluorescently tagged lectin to differentiate several species of *Pseudo-nitzschia* (Bacillophyceae) in Chinhae Bay, Korea. *Sci. Mar.* 65:207–14.

Coleman, A. W. 2009. Is there a molecular key to the level of "biological species" in eukaryotes? A DNA guide. *Mol. Phylogent. Evol.* 50:197–203.

Crooks, G. E., Hon, G., Chandonia, J. M. & Brenner, S. E. 2004. Weblogo: a sequence logo generator. *Genome Res.* 14:1188–90.

Dao, V. H., Omura, T., Takata, Y., Ky, P. X., Fukuyo, Y. & Kodama, M. 2012. *Pseudo-nitzschia* species, a possible causative

organism of domoic acid in *Spondylus versicolor* collected from Nha Phu Bay, Khanh Hoa Province, Vietnam. *Coast. Mar. Sci.* 35:7–10.

Dao, V. H., Takata, Y., Omura, T., Sato, S., Fukuyo, Y. & Kodama, M. 2009. Seasonal variation of domoic acid in a bivalve *Spondylus versicolor* in association with that in plankton samples in Nha Phu Bay, Khanh Hoa, Vietnam. *Fish. Sci.* 75:507–12.

Dao, V. H., Takata, Y., Sato, S., Fukuyo, Y. & Kodama, M. 2006. Domoic acid in a bivalve *Spondylus cruentus* in Nha Trang Bay, Khanh Hoa Province, Vietnam. *Coast. Mar. Sci.* 30:130–2.

Darty, K., Denise, A. & Ponty, Y. 2009. VARNA: interactive drawing and editing of the RNA secondary structure. *Bioinformatics* 25:1974–5.

Gottschling, M. & Plötner, J. 2004. Secondary structure models of the nuclear internal transcribed spacer regions and 5.8S rRNA in Calciodinelloideae (Peridiniaceae) and other dinoflagellates. *Nucleic Acid Res.* 32:307–15.

Hall, T. A. 1999. BioEdit: a user-friendly biological sequence alignment editor and analysis program for Windows 95/98/NT. *Nucleic Acids Symp. Ser.* 41:95–8.

Hasle, G. R. 1965. *Nitzschia* and *Fragilariopsis* species studied in the light and electron microscopes. *II. The group Pseudo-nitzschia. Skrift. Norske Vidensk. Akad.* 18:1–45.

Hasle, G. R. 2002. Are most of the domoic acid-producing species of the diatom genus *Pseudo-nitzschia* cosmopolites? *Harmful Algae* 1:137–46.

Huelsenbeck, J. P. & Ronquist, F. 2001. MRBAYES: Bayesian inference of phylogenetic trees. *Bioinformatics* 17:754–5.

Ichimura, T. & Kasa, F. 1995. Morphological variation and zygotic defective mating-type plus in a population of *Closterium ehrenbergii* (Desmidiales, Chlorophyta) from Boest Brook, Denmark. *Phycologia* 34:45–50.

Iwasaki, H. 1961. The life-cycle of *Porphyra tenera* in vitro. *Biol. Bull.* 121:173–87.

Keller, A., Förster, F., Müller, T., Dandekar, T., Schultz, J. & Wolf, M. 2010. Including RNA secondary structures improves accuracy and robustness in reconstruction of phylogenetic trees. *Biol. Direct.* 5:4.

Koetschan, C., Förster, F., Keller, A., Schleicher, T., Ruderisch, B., Schwarz, R., Müller, T., Wolf, M. & Schultz, J. 2009. The ITS2 Database III – sequences and structures for phylogeny. *Nucleic Acids Res.* 38:D275–9.

Koetschan, C., Förster, F., Keller, A., Schleicher, T., Ruderisch, B., Schwarz, R., Müller, T., Wolf, M. & Schultz, J. 2010. The ITS2 Database III – sequences and structures for phylogeny. *Nucleic Acids Res.* 38:D275–9.

Lelong, A., Hégaret, H., Soudant, P. & Bates, S. S. 2012. *Pseudo-nitzschia* (Bacillariophyceae) species, domoic acid and amnesic shellfish poisoning: revisiting previous paradigms. *Phycologia* 51:168–216.

Li, Y., He, L. N., Ma, Y. Y. & Lu, S. H. 2010. The study on morphological taxonomy of *Pseudo-nitzschia pseudodelicatissima* complex. *Acta Hydrobiol. Sin.* 34:302–11.

Lim, H. C. 2011. Morphological and molecular characterization of potential amnesic shellfish poisoning toxin-producing diatom *Pseudo-nitzschia* (Bacillariophyceae) from Malaysia. MSc dissertation, Faculty of Resource Science and Technology, Universiti Malaysia Sarawak, Malaysia, 153 pp.

Lim, H. C., Leaw, C. P., Su, S. N. P., Teng, S. T., Usup, G., Noor, N. M., Lundholm, N., Kotaki, Y. & Lim, P. T. 2012a. Morphology and molecular characterization of *Pseudo-nitzschia* (Bacillariophyceae) from Malaysian Borneo, including the new species *Pseudo-nitzschia circumpora* sp. nov. *J. Phycol.* 48:1232–47.

Lim, H. C., Lim, P. T., Su, S. N. P., Kotaki, Y. & Leaw, C. P. 2012b. Morphological observation of two species of *Pseudo-nitzschia* (Bacillariophyceae). *Coast. Mar. Sci.* 35:52–7.

Lim, H. C., Lim, P. T., Su, S. N. P., Teng, S. T. & Leaw, C. P. 2012c. Genetic diversity of *Pseudo-nitzschia brasiliana* (Bacillariophyceae) from Malaysia. *J. Appl. Phycol.* 24:1465–75.

Lundholm, N. [Ed.] *Bacillariophyta, in IOC-UNESCO Taxonomic reference list of harmful micro algae* 2011. Available at: http://www.marinespeceis.org/HAB (last accessed 28 December 2012).

Lundholm, N., Bates, S. S., Baugh, K. A., Bill, B. D., Connell, L. B., Léger, C. & Trainer, V. L. 2012. Cryptic and pseudo-cryptic diversity in diatoms-with descriptions of *Pseudo-nitzschia hasleana* sp. nov. and *P. fryxelliana* sp. nov. *J. Phycol.* 48:436–54.

Lundholm, N., Moestrup, Ø., Hasle, G. R. & Hoef-Emden, K. 2003. A study of the *Pseudo-nitzschia pseudodelicatissima/cuspidata* complex (Bacillariophyceae): what is *P. pseudodelicatissima*? *J. Phycol.* 39:797–813.

Lundholm, N., Moestrup, O., Kotaki, Y., Hoef-Emden, K., Scholin, C. & Miller, P. 2006. Inter- and intraspecific variation of the *Pseudo-nitzschia delicatissima* complex (Bacillariophyceae) illustrate by rRNA probes, morphological data and phylogenetic analyses. *J. Phycol.* 42:464–81.

Mai, J. C. & Coleman, A. W. 1997. The internal transcribed spacer 2 exhibits a common secondary structure in green algae and flowering plants. *J. Mol. Evol.* 44:258–71.

Mathews, D. H., Disney, M. D., Childs, J. L., Schroeder, S. J., Zuker, M. & Turner, D. H. 2004. Incorporating chemical modification constrains into a dynamic programming algorithm for prediction of RNA secondary structure. *Proc. Natl Acad. Sci. USA* 101:7287–92.

McDonald, S. M., Sarno, D. & Zingone, A. 2007. Identifying *Pseudo-nitzschia* species in natural samples using genus-specific PCR primers and clone libraries. *Harmful Algae* 6:849–60.

Moschandreou, K. K., Baxevanis, A. D., Katikou, P., Papaefthimiou, D., Nikolaidis, G. & Abatzopoulos, T. J. 2012. Inter- and intra-specific diversity of *Pseudo-nitzschia* (Bacillariophyceae) in the northeastern Mediterranean. *Eur. J. Phycol.* 47:321–39.

Moschandreou, K. K. & Nikolaidis, G. 2010. The genus *Pseudo-nitzschia* (Bacillariophyceae) in Greek coastal waters. *Bot. Mar.* 53:159–72.

Müller, T., Philippi, N., Dandekar, T., Schultz, J. & Wolf, M. 2007. Distinguishing species. *RNA* 13:1469–72.

Notredame, C., Higgins, D. G. & Heringa, J. 2000. T-Coffee: a novel method for fast and accurate multiple sequence alignment. *J. Mol. Biol.* 302:205–17.

Orive, E., Laza-Martinez, A., Seoane, S., Alonso, A., Andrade, R. & Miguel, I. 2010. Diversity of *Pseudo-nitzschia* in the Southeastern Bay of Biscay. *Diatom Res.* 25:125–45.

Orsini, L., Procaccini, G., Sarno, D. & Montresor, M. 2004. Multiple rDNA ITS-types within the diatom *Pseudo-nitzschia delicatissima* (Bacillariophyceae) and their relative abundances across a spring bloom in the Gulf of Naples. *Mar. Ecol. Prog. Ser.* 271:87–98.

Peculis, B. A. & Greer, C. L. 1998. The structure of the ITS2-proximal stem is required for pre-rRNA processing in yeast. *RNA* 4:1610–22.

Posada, D. 2008. jModelTest: phylogenetic model averaging. *Mol. Biol. Evol.* 25:1253–6.

Quijano-Scheggia, S., Garcés, E., Andree, K. B., Iglesia, P. D. L., Diogène, J., Fortuño, J. M. & Camp, J. 2010. *Pseudo-nitzschia* species on the Catalan coast: characterization and contribution to the current knowledge of the distribution of this genus in the Mediterranean Sea. *Sci. Mar.* 74:395–410.

Quijano-Scheggia, S. I., Garcés, E., Lundholm, N., Moestrup, Ø., Andree, K. B. & Camp, J. 2009. Morphology, physiology, molecular phylogeny and sexual compatibility of the cryptic *Pseudo-nitzschia delicatissima* complex (Bacillariophyta), including the description of *P. arenysensis* sp. nov. *Phycologia* 48:492–509.

Ruhl, M. W., Wolf, M. & Jenkins, T. M. 2010. Compensatory base changes illuminate morphologically difficult taxonomy. *Mol. Phylogent. Evol.* 54:664–9.

Scholin, C. A., Herzog, M., Sogin, M. & Anderson, D. M. 1994. Identification of group- and strain-specific genetic markers for globally distributed *Alexandrium* (Dinophyceae). II. Sequence analysis of a fragment of the LSU rRNA gene. *J. Phycol.* 30:999–1011.

Schultz, J., Müller, T., Achtziger, M., Seibel, P. N., Dandekar, T. & Wolf, M. 2006. The internal transcribed spacer 2 database-

a web server for (not only) low level phylogenetic analyses. *Nucleic Acids Res.* 34:W704–7.
Seibel, P. N., Müller, T., Dandekar, T., Schultz, J. & Wolf, M. 2006. 4SALE – a tool for synchronous RNA sequence and secondary structure alignment and editing. *BMC Bioinformatics* 7:498.
Seibel, P. N., Müller, T., Dandekar, T. & Wolf, M. 2008. Synchronous visual analysis and editing of RNA sequence and secondary structure alignments using 4SALE. *BMC Res. Notes* 1:91.
Selig, C., Wolf, M., Müller, T., Dandekar, T. & Schultz, J. 2008. The ITS2 Database II: homology modelling RNA structure for molecular systematic. *Nucleic Acids Res.* 36:D377–80.
Su, S. N. P. 2011. Ecology and taxonomy of amnesic shellfish poisoning (ASP) diatom *Pseudo-nitzschia* species (Bacillariophyceae) in Malaysian waters. MSc dissertation, Faculty of Resource Science and Technology, Universiti Malaysia Sarawak, Malaysia, 134 pp.
Swofford, D. L. 2001. *PAUP*. Phylogenetic Analysis Using Parsimony (*and other methods). Version 4.* Sinauer Associates, Sunderland, MA.
Takata, Y., Sato, S., Ha, D. V., Montojo, U. M., Lirdwitayaprasit, T., Kamolsiripichaiporn, S., Kotaki, Y., Fukuyo, Y. & Kodama, M. 2009. Occurrence of domoic acid in tropical bivalves. *Fish. Sci.* 75:473–80.
Talavera, G. & Castresana, J. 2007. Improvement of phylogenies after removing divergent and ambiguously aligned blocks from protein sequence alignments. *Syst. Biol.* 56:564–77.
Teng, S. T., Leaw, C. P., Lim, H. C. & Lim, P. T. 2013. The genus *Pseudo-nitzschia* (Bacillariophyceae) in Malaysia, including new records and a key to species inferred from morphology-based phylogeny. *Bot. Mar.* doi:10.1515/bot-2012-0194.
Trainer, V. L., Bates, S. S., Lundholm, N., Thessen, A. E., Cochlan, W. P., Adams, N. G. & Trick, C. G. 2012. *Pseudo-nitzschia* physiological ecology, phylogeny, toxicity, monitoring and impacts on ecosystem health. *Harmful Algae* 14:271–300.
Trainer, V. L., Wells, M. L., Cochlan, W. P., Trick, C. G., Bill, B. D., Baugh, K. A., Beall, B. F., Herndon, J. & Lundholm, N. 2009. An ecological study of a massive bloom of toxigenic *Pseudo-nitzschia cuspidata* off the Washington State coast. *Limnol. Oceanogr.* 54:14.
Vrieling, E. G., Koeman, R. P. T., Scholin, C. A., Scheerman, P., Peperzak, L., Veenhuis, M. & Gieskes, W. W. C. 1996. Identification of a domoic acid-producing *Pseudo-nitzschia* species (Bacillariophyceae) in the Dutch Wadden Sea with electron microscopy and molecular probes. *Eur. J. Phycol.* 31:333–40.
White, T. J., Bruns, T., Lee, S. & Taylor, J. W. 1990. Amplification and direct sequencing of fungal ribosomal RNA genes for phylogenetics. *In* Innis, M. A., Gelfand, D. H., Sninsky, J. J. & White, T. J. [Eds.] *PCR Protocols: A Guide to Methods and Applications.* Academic Press Inc., San Diego, CA, pp. 315–22.
Wiemers, M., Keller, A. & Wolf, M. 2009. ITS2 secondary structure improves phylogeny estimation in a radiation of blue butterflies of the subgenus *Agrodiaetus* (Lepidoptera: Lycaenidae: *Polyommatus*). *BMC Evol. Bio.* 9:300.

Supporting Information

Additional Supporting Information may be found in the online version of this article at the publisher's web site:

Appendix S1. Sequence alignment of ITS1-5.8S-ITS2, LSU rDNA and ITS2 (sequence-structural information) used in this study.

Table S1. Strain designation, localities and date when samples were collected for cultures of *Pseudo-nitzschia* established for this study. (* indicates sequence obtained from type strains; bold indicates strains obtained in this study).

Table S2. Morphometric data of *Pseudo-nitzschia batesiana*, *P. lundholmiae*, and *P. fukuyoi* compared to its closest species. Brackets indicate number of cells measured in this study.

Table S3. List of ITS-5.8S-ITS2 and LSU rDNA sequences of *Pseudo-nitzschia* used in phylogenetic studies. (* indicates sequence obtained from type strains; bold indicates strains obtained in this study).

Table S4. Corrected *p*-distances (%) of *Pseudo-nitzschia batesiana*, *P. lundholmiae*, and *P. fukuyoi* for the ITS2 data set (upper diagonal) and LSU rDNA data set (lower diagonal) compared to their closely related species.

Table S5. Numerical and statistical values of the secondary structures (ITS2) of selected *Pseudo-nitzschia* species; * indicates the type strains, bold indicated the strains obtained in this study.

Table S6. Comparisons of the secondary structures of *Pseudo-nitzschia batesiana*, *P. lundholmiae*, and *P. fukuyoi* to its closely related species.